Biochimica et Biophysica Acta, 1029 (1990) 285–294
Elsevier

BBAMEM 75038

The influence of physical characteristics of liposomes containing doxorubicin on their pharmacological behavior

D. Goren [1,2], A. Gabizon [1], and Y. Barenholz [2]

[1] *Department of Oncology, Hadassah University Hospital, Jerusalem and* [2] *Department of Membrane Biochemistry, Hebrew University - Hadassah Medical School, Jerusalem (Israel)*

(Received 19 February 1990)
(Revised manuscript received 26 July 1990)

Key words: Liposome; Vesicle size; Oligolamellar vesicle; Small unilamellar vesicle; Doxorubicin; Drug entrapment

We have investigated the behavior of two populations of doxorubicin (DXR)-containing phospholipid vesicles with regard to various physical and pharmacological parameters. DXR-containing liposomes were prepared by ultrasonic irradiation, the lipid composition being phosphatidylglycerol (or phosphatidylserine), phosphatidylcholine and cholesterol. The vesicles were fractionated into oligolamellar vesicles (OLV) and small unilamellar vesicles (SUV) by preparative differential utracentrifugation (150 000 × *g* for 1 h). Unentrapped DXR was removed by gel exclusion chromatography. OLV and SUV liposomes differed in size (mean diameters, 247 ± 113 nm and 61 ± 16 nm, respectively) and number of lamellae (two for OLV, one for SUV). Drug entrapment per unit of lipid was three to 5-fold higher in OLV than in SUV. In both liposome populations more than 95% of the entrapped drug was membrane-associated. Physical studies on these two vesicle populations revealed higher motional restriction and greater susceptibility to iodide-mediated fluorescence collisional quenching of DXR in the small vesicles. OLV showed superior stability in the presence of plasma as determined by the fraction of DXR retained by the vesicles. It was also found that the tissue distribution of DXR in SUV follows a pattern different from that of DXR in OLV and resembling that of soluble DXR. In accordance with these differences in patterns of tissue distribution, animal studies demonstrated that DXR in OLV is significantly less toxic than DXR in SUV and more effective in a tumor model with predominant involvement of the liver. These results indicate that vesicle size and/or number of lamellae play an important role in optimizing liposome-mediated delivery of DXR, and that oligolamellar liposomes are distinctively superior to small unilamellar liposomes when fluid phase formulations (T_m < 37 °C) with bilayer-associated DXR are considered.

Introduction

The use of liposomes as doxorubicin (DXR) carriers in cancer chemotherapy offers a potential means to improve the drug therapeutic index. Cardiotoxicity, a major clinical handicap limiting DXR cumulative dosage is reduced, while the therapeutic activity is increased or preserved in a variety of experimental tumor models [1–7].

In previous work, we have optimized liposome composition for DXR delivery [8,9] according to the following criteria: high efficiency of drug capture; preservation of the full in vitro cytotoxic activity of the encapsulated drug; stability in the presence of plasma; favorable tissue distribution pattern, as indicated by reduced uptake of liposome-associated DXR by the heart muscle and higher drug levels in the liver; decreased toxicity; and increased therapeutic activity in various relevant tumor models.

Besides the selection of lipid composition, another factor in determining the biodistribution and pharmacokinetic profile, is vesicle size. Extensive work from several laboratories point at liposome size as a key factor in the in vivo behavior of liposomes and therefore an important element in the design of a drug delivery system [10,11]. In general, the smaller the liposome size,

Abbreviations: CHOL, cholesterol; DXR, doxorubicin; F-DXR, free doxorubicin; L-DXR, liposome-associated doxorubicin; MLV, multilamellar vesicles; OLV, oligolamellar vesicles; PC, phosphatidylcholine; PE, phosphatidylethanolamine; PG, phosphatidylglycerol; RES, reticuloendothelial system; SUV, small unilamellar vesicles; TLC, thin-layer chromatography; TNBS, trinitrobenzenesulfonic acid; TNP-PE, trinitrophenylphosphatidylethanolamine.

Correspondence: A. Gabizon, Department of Oncology, Hadassah University Hospital, P.O. Box 12000, Jerusalem 91120, Israel.

the longer the circulation time in blood. With regard to intrahepatic distribution, several reports indicate that small unilamellar vesicles (SUV) can penetrate the sinusoid fenestrations and reach hepatocytes, while large multilamellar vesicles (MLV) localize exclusively in Kupffer cells [10,12,13]. To achieve liposome delivery to extravascular targets, such as solid tumors, prolongation of the presence of intact liposomes in the circulation, seems to be an important requirement [14]. In that respect, small liposomes would be the appropriate vesicles for drug delivery [10]. However, vesicle size has also a major impact on the liposome physical properties [15] which may affect drug–lipid interaction and/or drug release from the vesicles. In addition, the therapeutic effect of liposome-associated DXR may stem from drug and active metabolites release by the reticulo-endothelial system (RES) following phagocytosis and processing of liposomes [16]. It was therefore of interest to test in a comparative study SUV and larger liposomes to determine the optimal size and number of lamellae for a DXR-carrying vesicle, and to examine the contribution of the physical properties of liposomes to their pharmacological properties. Since sterility procedures would generally require liposomes to be ultrafilterable, we decided to perform these studies on liposomes with an average size below 300 nm.

Materials and Methods

(A) Preparation of liposomes

High purity phospholipid batches (99%) were obtained from Lipid Products (Surrey, U.K.) and Avanti Polar Lipids (Birmingham, AL). Cholesterol (Chol) standard for chromatography and α-tocopherol succinate were obtained from Sigma (St. Louis, MO). DXR (vials containing 50 mg doxorubicin HCl and 250 mg lactose) was obtained from Farmitalia-Carlo Erba (Milan, Italy). For preparation of the liposomes, the lipids phosphatidylglycerol (PG), phosphatidylcholine (PC), Chol and α-tocopherol succinate were mixed in a round bottom flask at a molar ratio of 3 : 7 : 4 : 0.2, and the lipid solvents were evaporated under vacuum with a rotary evaporator. In some of the initial experiments, phosphatidylserine replaced PG. In most experiments DXR (5 $mg \cdot ml^{-1}$) in unbuffered 0.9% NaCl solution (pH 6.0 ± 0.5), was added to the dried lipid film to a final concentration of 15 to 40 $\mu mol \cdot ml^{-1}$ phospholipid. In order to avoid the effect of metal ions on the liposome preparation, especially ferric ions, 50 μM deferoxamine mesylate (Desferal, Ciba-Geigy, Basel, Switzerland) were added to the saline solution used along all steps of liposome preparation. This solution is referred to as saline-desferal. The lipid film was hydrated by vortexing, following by shaking to form multilamellar vesicles. These were subsequently submitted to pulsed ultrasonic irradiation with a probe sonicator (W-225, Heat Systems Ultrasonics, Plain View, NY), equipped with a saphire bottom to reduce metal contamination. Ultrasonic irradiation was carried out for 5 to 20 min, at 4° C under a continuous nitrogen flow. This process produced vesicles of broad size distribution from which two vesicle populations were fractionated by differential ultracentrifugation ($150\,000 \times g$ for 1 h) [17]. The relative yield of each population was affected by various aspects of the ultrasonication process, such as time, suspension volume, lipid concentration, and shape of vial used [15,17]. SUV were collected in the supernatant. OLV were recovered by resuspension of the pellet in saline-desferal. Both types of liposomes were separated from free DXR by Sephadex G-50 gel filtration [8]. The liposomal preparations were stored at 4° C in siliconized vacuum sealed tubes (Vacutainer Systems, Rutherford, NY) proteced from light, and were used within three weeks.

Stability studies indicate that the combined protection by desferal and α-tocopherol succinate was effective and superior over the α tocopherol-desferal combination in reducing chemical degradation of either lipids and especially DXR during vesicle preparation and the storage period required for experimental testing [46]. Lipid perodixation [15,18] was not significantly different from the baseline level in the raw materials. The level of lysophospholipid derivatives [15] did not exceed 2.0%. DXR degradation [19–21] was below 5%. Increase in size due to aggergation and/or fusion was followed by measurements of specific turbidity at 650 nm, a wavelength at which DXR absorbance is minimal. OLV appeared to be more physically stable than SUV. Preparations that showed an increase in specific turbidity during storage were not used in this study.

(B) Liposome characterization

(B1) Doxorubicin concentration

DXR content of the liposomes was determined fluorometrically in liposome samples dissolved in acidified ethanol (0.3 M HCl in 50% ethanol) or acidified isopropanol (0.075 M HCl in 90% isopropanol) using a Perkin-Elmer MPF-44 spectrofluorometer (excitation: 480 nm; emission: 590 nm). Fluorescence intensity was translated to DXR equivalents, using standard curves of DXR. Alternatively, DXR concentration was determined by dissolving the liposomes in the above acidified isopropanol and measuring the absorbance at 480 nm spectrophotometrically. The concentration was calculated based on an extinction coefficient of 12 500 $A\ unit \cdot M^{-1} \cdot cm^{-1}$.

(B2) Phospholipid concentration

Phospholipid concentration was determined according to either a phosphorus Bartlett assay [22] or a colorimetric determination with ammonium ferrothyocyanate [23] using PC/PG (7 : 3, mole/mole) as standard curve. The assay was done under acidic conditions (0.1 M HCl) which enable complete dissociation between PG and DXR.

(B3) Liposome phospholipid composition

OLV and SUV lipids were extracted by Bligh and Dyer procedure [27]. Aliquots of the chloroformic lower phase were loaded on 0.25 mm silica gel G uniplate (Analtech, Newark, U.S.A.) and a solvent system of chloroform/ acetone/ methanol/ glacial acetic acid/ water (6 : 8 : 2 : 2 : 1, by vol.) was used. The following R_f values were obtained: PG, 0.53; PC, 0.13. The spots of PG and PC were scraped for phosphorus analysis [22].

(B4) Size determination

Size distribution measurements of the vesicles were done by quasi-elastic light scattering (QELS) [15] using a Malvern 4700 submicron particle analyzer (Malvern Instruments, Worcestershire, U.K.).

(B5) Trapped volume determination

The trapped volume of the DXR-vesicles was determined by entrapping [^{3}H]inulin (Amersham, U.K.) in the vesicles during their preparation [15,24]. The nonentrapped inulin was removed from the liposomes using Sepharose 6B column (Pharmacia). The ratio of radioactivity (inulin content) to phospholipid content [22] was determined before and after the gel exclusion chromatography and was used to calculate the trapped aqueous volume [15,24].

(B6) Determination of average number of vesicle lamellae

The average number of vesicle lamellae was determined by chemical labeling of a marker phospholipid (phosphatidylethanolamine, PE) with trinitrobenzenesulfonate (TNBS), a membrane impermeable reagent [17,25,26]. PE was prepared by transphosphatidylation of egg PC with phospholipase D and was therefore of a similar acyl chain composition to egg PC and egg-derived PG used for liposome preparation. The lipid composition of the formulation was modified by including 10 mole % PE per total phospholipid. Vesicles were prepared and fractionated as described above. The two vesicle populations were then reacted with TNBS.

For unilamellar vesicles, the mole percent of exposed PE should reflect the lipid mass distribution between the two leaflets, which is dependent on vesicle size [15]. For large unilamellar vesicles it should approach a minimal value of 50%. Reducing the vesicle size increases the curvature and therefore increases the ratio of lipid in the outer leaflet over the lipid in the inner leaflet (out/in ratio), until it reaches a value close to 2 (66%/33%) [15,17,25,26]. Increasing the number of lamellae reduces the % PE exposed to below 50% (i.e., for two lamellae per vesicle in average, only 25% of PE should be labelled by TNBS). The average number of lamellae is estimated from the mole% of PE reacting with (TNBS) to give trinitrophenyl-PE (TNP-PE) as described elsewhere [15]. Lipids including TNP-PE were extracted by the acidic Bligh and Dyer procedure [27]. TNP-PE content was determined spectrophotometrically at 350 nm. The calculation is based on the following formula:

$$\%\ \text{PE exposed} = \frac{\text{TNP-PE in intact vesicles}}{\text{total TNP-PE in solubilized vesicle}}$$

The extracted lipids of the solubilized vesicles used to obtain total PE were analyzed by thin-layer chromatography. Precoated TLC aluminium sheets of silica gel 60 were used. Separation was carried out as described before (under (B3) Liposome phospholipid composition). Only TNP-PE (R_f 0.87) but no free PE (R_f 0.47) was observed. This proves that indeed all PE was labelled in the solubilized vesicles.

DXR, which has a primary amino group on its daunosamine moiety, also forms a TNP-DXR derivative (R_f 0.93 in the above TLC analysis). However, due to the excess of TNBS in the reaction, this did not interfere with PE labelling.

(C) DXR organization in the vesicles

Three different fluorescent properties of DXR were used to characterize DXR organization in the vesicles: (1) self-quenching, (2) collisional quenching, and (3) steady-state fluorescence anisotropy.

(C1) Self quenching

Self-quenching is dependent on the concentration of the fluorophore in a given system. Release of self-quenching (dequenching) is obtained through liposome solubilization in acidic isopropanol (0.075 M HCl in 90% isopropanol). The fluorescence intensity at 590 nm (F_{590}) was determined in saline-desferal and acidic isopropanol in order to correct for the increase in the fluorescence intensity which is related to the decrease in medium dielectric constant. In these experiments, the concentration of DXR, either as F-DXR or L-DXR, was always below $1 \cdot 10^{-5}$ M to eliminate self-association [28]. The degree of self-quenching was calculated as follows:

$$\%\ \text{quenching} = 100 - \frac{\dfrac{F_{590}\ \text{isopropanol}}{F_{590}\ \text{saline}}\ \text{F-DXR}}{\dfrac{F_{590}\ \text{isopropanol}}{F_{590}\ \text{saline}}\ \text{L-DXR}} \times 100$$

(C2) Collisional quenching

Collisional quenchers such as iodide which are membrane impermeable are used to assess fluorophore availability [19,25,29,30]. The quenching mechanism and efficiency is determined from the Stern-Volmer plots in which:

$$\frac{F_0}{F} = 1 + K_{SV}[Q]$$

The Stern Volmer coefficient (K_{SV}) is the slope of the curve; F_0 and F are the fluorescence intensities in the absence and presence of the quencher (Q), respectively. Linear relationships in the Stern-Volmer plots are indicative of a dynamic quenching process. Nonlinearity in the Stern-Volmer plots suggests a combination of dynamic and static quenching processes which can be separated by using the modified equation [30,31]:

$$\frac{F_0}{F_{v(Q)}} = 1 + K_{SV}[Q]$$

The quenching studies were carried out at 23° C in saline-desferal, in the presence of potassium iodide (0.1–0.5 M KI) and 2 mM of sodium thiosulfate to prevent iodide oxidation. DXR concentration was $1 \cdot 10^{-6}$–$4 \cdot 10^{-6}$ M. In some experiments $KClO_4$ (a non-quencher salt) was added to keep the osmolality constant. Fluorescence emission spectra were unaltered by iodide. Degree of quenching was calculated from the intensity of fluorescence emission at 590 nm (excitation, 480 nm).

(C3) Steady-state fluorescence anisotropy

Steady-state fluorescence anisotropy of DXR was used to monitor its rotational diffusion. This parameter is affected by a combination of structural hindrance to the extent and rate of rotation [29,32]. Steady-state fluorescence anisotropy (r) was determined using a Perkin-Elmer MPF-44 in L format equipped with a polarization unit described elsewhere [33]. All measurements were performed in saline-desferal with a DXR concentration of $1 \cdot 10^{-6}$–$4 \cdot 10^{-6}$ M, and at a temperature range of 20–50° C with intervals of 1 C°.

(D) Pharmacological aspects

(D1) Plasma stability studies

For this, liposome samples (2.5 μmol phospholipids/ml) were incubated for 1 h at 37° C in the presence of 50% of human plasma, using a shaker water bath. Separation of released drug from the liposomal bound form of DXR was performed by Sephadex G-50 size exclusion chromatography. We found that during this incubation 25% of the free doxorubicin binds to plasma proteins and lipoproteins over a range of 0.4–2.0 mM DXR and is eluted from the Sephadex column in the void volume together with liposome-associated DXR. Therefore, the amount of liposomal DXR was obtained by substracting the protein- and lipoprotein-associated DXR from the doxorubicin in the void volume according to the following equation:

$$DXR_{liposomal} = DXR_{void} - (0.33.DXR_{free})$$

The validity of these determinations was confirmed recently by replacing the Sephadex G-50 with Bio-Gel A15 which separates liposomal DXR from protein-bound DXR [21].

(D2) In vivo studies

Age and sex-matched syngeneic BALB/c mice, from the animal breeding center of the Hebrew University, Jerusalem, Israel, were used.

Tissue distribution studies. Mice were given injections through the tail vein of equivalent amounts of DXR (10 mg/kg), in either free or liposome entrapped form, OLV and SUV. The corresponding phospholipid dose was approx. 2 μmol per mouse for OLV, and 6 μmol for SUV. At the specified time intervals after injection, the animals were killed by cervical dislocation and the liver, spleen, lungs, kidneys, intestine and heart were rapidly excised, rinsed in 0.9% NaCl solution and stored at −70° C. DXR content was measured in organs pooled from three mice for each time point tested. DXR was extracted according to the method of Bachur et al. [34]. Shortly after thawing, tissues were weighed, homogenized in acidified ethanol with a high speed omnimixer for 3 min, and centrifuged at $20000 \times g$ for 20 min. Tissues from noninjected mice, treated by the same procedure, served as blank. DXR fluorescence was measured in the supernatant as described previously [8]. Each time point value is the mean of data obtained from three mice. S.D. did not exceed 15%. The significance of the differences between the means of the experimental groups along the various time points was analyzed by the paired t-test.

Toxicity. Toxicity experiments were performed in BALB/c male mice using a single i.v. injection of escalated doses of DXR in free or liposome encapsulated form (OLV and SUV). Five animals were tested at each dose level.

Efficacy. Tumor cells were obtained from a BALB/c radiation induced T-cell derived lymphoma (J-6456) described previously [35]. For therapy experiments, J-6456 lymphoma cell suspensions were prepared aseptically by trypsinization of minced pieces of the tumor (0.25% trypsin, GIBCO, New York, NY) and washing with RPMI medium (GIBCO). The viability of the cell preparation as determined by the trypan blue exclusion test, was 95%. Hepatosplenic metastases were produced by i.v. injection of 10^6 J-6456 cells in syngeneic BALB/c

mice [6]. Three i.v. injections of 8 mg DXR/kg in either free (F-DXR), SUV-associated, or OLV-associated form were given on days 3, 10 and 17 after tumor cell injection. Mice were inspected daily and survival curves recorded. The increase in median life span was calculated as:

$$\frac{T \times 100}{C} - 100$$

where T and C are the median life spans of the treated and untreated control groups, respectively.

Results

(A) Liposome characterization

Analysis of phospholipid composition of SUV and OLV revealed that both are almost identical in their PC/PG molar ratio (2.55 and 2.43, respectively). The difference in mean size distribution of each of the two vesicle populations obtained after ultrasonic irradiation and ultracentrifugation was in the range of 3–4-fold (Table I). The SUV population was monodisperse with a rather small standard deviation for the distribution mean. In the OLV population the distribution was polydisperse with a large standard deviation (Table I), and in some cases bimodal (Fig. 1). In all cases there was almost no overlap between the distribution range of OLV and SUV (Fig. 1).

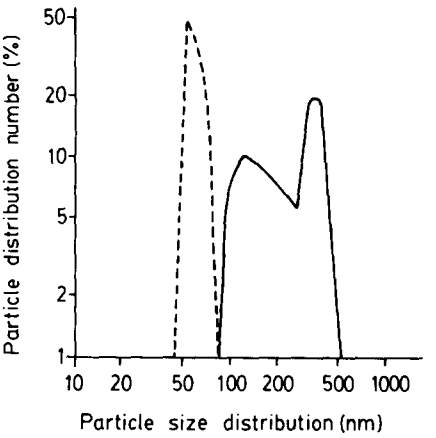

Fig. 1. Particle size distribution. - - - - - -, SUV; ———, OLV.

TABLE I

Comparison of structural parameters of SUV-DXR and OLV-DXR

Liposomes were prepared as described in Materials and Methods using 17.2 mM phospholipids and 3.5 mM DXR (input mole ratio of DXR to phospholipid = 0.20).

	SUV	OLV
Mean size [a] (diameter, nm)	61.0 ± 16	247.0 ± 113
% External phospholipids [b]	45.9 ± 2.5	25.0 ± 1.8
Estimated average number of bilayers [b]	1.0	2.0
Liposome-associated DXR (nmol DXR/μmol phospholipid)	65.0 ± 20	260.0 ± 50
V_t [c] (μl/μmol phospholipid)	0.4	1.2
DXR in liposome aqueous phase [d] (nmol DXR/μmol phospholipid)	1.4	4.3
% of total DXR in liposome aqueous phase [e]	3.1	1.7

[a] Based on QELS analysis using Malvern 4700C system.

[b] Determined by the TNBS assay (see Materials and Methods). For the OLV, this is the minimal number of lamellae present if the internal bilayer is adjacent to the external. When the internal bilayers are closer to the vesicle center each bilayer will be composed of less lipid molecules and therefore, the total number of lamellae may be underestimated.

[c] V_t (trapped aqueous volume) was calculated as described in Materials and Methods using [^{3}H]inulin as marker for aqueous phase entrapment.

[d] Theoretical maximal amount of DXR in liposome aqueous phase calculated from V_t of [^{3}H]inulin.

[e] Calculated from the total liposome associated DXR and from point d.

According to the TNBS labeling method (Table I), the smaller vesicles are unilamellar and therefore are referred to as SUV while the larger liposomes have, on the average, two lipid bilayers (see footnote b, Table I). Therefore the large vesicles are referred to as oligolamellar vesicles (OLV). Our findings that these vesicles are made up of several bilayers were confirmed by negative staining electron microscopy (data not shown).

It is obvious from Table I that the larger size liposomes (OLV) have a much greater drug-carrying capacity for DXR than SUV. For the same amount of phospholipid, the DXR content is 3–5-fold higher in the OLV (Table I). It should also be noted that the relative difference in loading capacities (final DXR/phospholipid mole ratio) of OLV and SUV are almost unaffected by the initial (input) DXR to phospholipid mole ratio in the range of input ratio 0.08–0.24. These results are in agreement with previous studies comparing MLV with SUV [8], and OLV with SUV [36], in both of which SUV had a smaller drug-loading capacity.

Using [^{3}H]inulin we determined the aqueous trapped volume and therefore the maximal amount of DXR that may be entrapped in the aqueous phase of the two types of vesicles (Table I). The results indicate that, at the most, 3.1% and 1.7% of the entrapped DXR is in the aqueous phase of SUV and OLV, respectively. Namely, in both populations, above 95% of the entrapped DXR is membrane-associated.

(B) DXR organization in the vesicles

(B1) DXR self-quenching

Liposomes were prepared as described in Methods, using input ratio of DXR to phospholipids of 0.08 (mole/mole). SUV and OLV were separated by differential centrifugation. The output ratio in the liposomes were 0.021 and 0.078 for the SUV and OLV, respectively. Self-quenching was then determined as described in Materials and Methods. DXR self-quenching in the OLV was much greater than in the SUV, 62% and 7%, respectively.

(B2) Collisional quenching

Fig. 2 shows Stern-Volmer plots of DXR quenching by iodide, a membrane-impermeable collisional quencher, for SUV, OLV and F-DXR. The Stern-Volmer plot for free DXR shows deviation from linearity. This suggests the involvement of static quenching in addition to the dynamic process [25,31]. However, there is no indication for the involvement of static process in the quenching of DXR in either SUV or OLV since for both the Stern-Volmer plots are linear. K_{SV} determined from the plots show a distinct difference between the two liposome populations (K_{SV} of 1.6 M^{-1} for OLV – DXR; and, K_{SV} of 10.8 M^{-1} for SUV-DXR). Very similar results were obtained at constant osmolality which was achieved by adding the desired concentration of the nonquencher salt $KClO_4$. Although the possibility that the major part of the DXR in OLV is in the aqueous phase of the liposome can be ruled out from

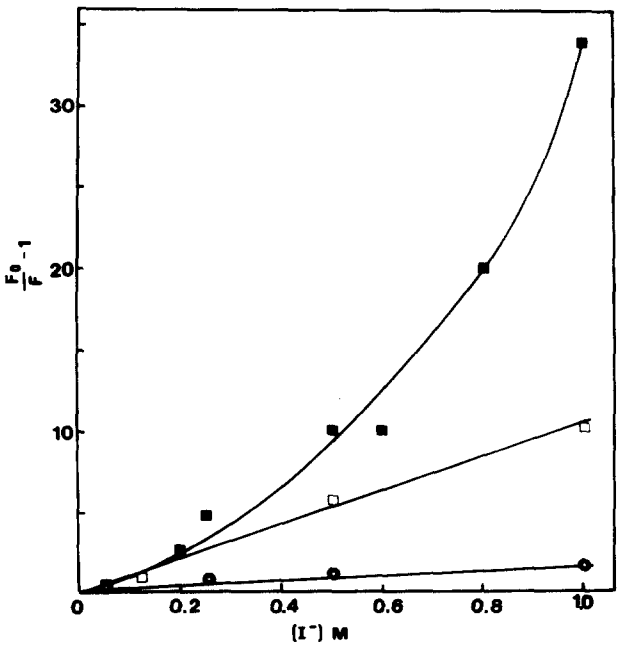

Fig. 2. Stern-Volmer plots for iodide quenching of DXR fluorescence: Comparison between free-DXR (■), SUV-DXR (□), and OLV-DXR (○) in saline-desferal.

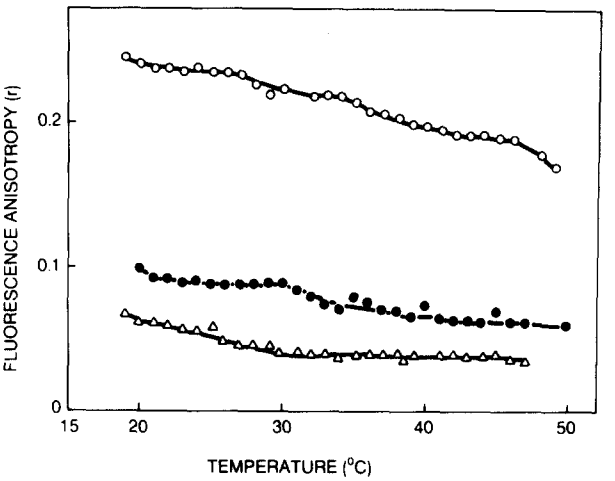

Fig. 3. Temperature-dependent (20°-50°C) steady-state fluorescence anisotropy of free-DXR (△), OLV-DXR (●) and SUV-DXR (○).

the trapped volume data (Table I), we further tested this by rupturing the liposomes by osmotic shock with a 1 : 100 dilution step in double-distilled H_2O and repeating the quenching experiments. Increase of K_{SV} is expected if DXR is released into the external medium. However, this was not the case, and actually K_{SV} was reduced by factor of 1.4 after the osmotic shock, suggesting that DXR was not released into the external medium. This reduction in K_{SV} is as yet unexplained, although it suggests reduction in DXR accessibility to the quencher. The results of the above experiment were confirmed by finding that almost no free drug was released into the medium after osmotic shock, based on gel exclusion chromatography.

(B3) Rotational mobility of DXR

The restriction to the rotational motion of DXR was determined from its steady-state fluorescence anisotropy. The temperature dependent steady-state fluorescence anisotropy (r) curves for F-DXR, OLV-DXR and SUV-DXR (Fig. 3) are smooth, suggesting that liposomal DXR does not monitor a phase change. As expected for this lipid composition, the bilayer is in the liquid ordered phase [37] throughout the temperature range of 25–50°C. Based on limiting anisotropy defined as r_0 [29] of 0.39 [31], free DXR in saline-desferal is highly mobile (r at 25°C = 0.05). In SUV the rotational motion of DXR is highly restricted as the fluorescence anisotropy of DXR in SUV is very high (r at 25°C = 0.23). The r values of free DXR and DXR in SUV resemble the r values obtained previously in a study in which free DXR was compared with DXR associated with dimyristoylphosphatidylcholine SUV in their liquid state [31]. Interestingly, fluorescence anisotropy values of DXR in OLV are much lower and varied between 0.07 to 0.1 in the temperature range of 50 to 20°C, respectively. As with the quenching experi-

ments, the possibility that a major part of the DXR in OLV is present in the aqueous compartment of the liposome, thus contributing to a decrease in r values, was discarded by the data on trapped volume and by osmotic shock experiments.

(C) Pharmacological aspects

(C1) Stability of liposomes in plasma

One of the essential requirements for the use of liposomes as in vivo carriers is their ability to retain the entrapped drug in the presence of whole blood or its constituents. We studied the release of DXR from SUV and OLV (for details see Methods). OLV were more stable that SUV, their drug release never exceeding 45%. SUV showed marked lability, releasing up to 85% of the vesicle-associated drug.

(C2) Tissue distribution studies

Fig. 4 shows the concentrations of DXR in liver, spleen, kidney and heart, after bolus injection of 10 mg/kg of either F-DXR or DXR entrapped in OLV or SUV liposomes. The levels of DXR in liver and spleen were markedly increased by delivery with OLV. The increasing difference in liver drug concentration at 5 and 24 h after injection is probably due to slower clearance of the OLV-associated drug, since by 1 h after injection plasma drug levels are too low to account for any significant uptake by the liver. SUV caused a smaller increase than OLV in the drug accumulating in liver and spleen. Examination of other organs, such as heart, kidneys (Fig. 4), lungs and small intestine (data not shown) indicates the following order of accumulation: F-DXR > SUV-DXR > OLV-DXR. These results are in agreement with the marked instability of SUV-DXR and their much higher DXR leakage rate in plasma.

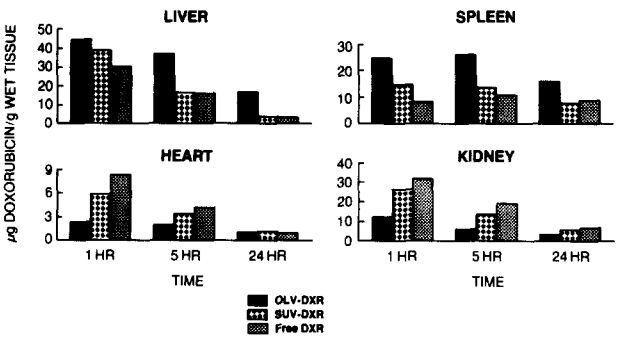

Fig. 4. A comparison of the tissue distribution of DXR in free-, OLV- and SUV-associated forms: Mice were given injections of 10 mg/kg of DXR in either free or liposome entrapped form. Liver, spleen, heart and kidney were excised at the time points shown. DXR amount was assayed as described in Materials and Methods. Statistical analysis using the paired t test: OLV-DXR vs. SUV-DXR, $P = 0.046$ for liver, $P = 0.016$ for spleen; OLV-DXR vs. Free DXR, $P = 0.022$ for liver, $P = 0.047$ for spleen. Differences between SUV-DXR and Free-DXR were not significant.

(C3) Toxicity of liposome-associated and free DXR

Table II shows the survival of mice injected with F-DXR, OLV-DXR, and SUV-DXR. Both liposome preparations reduced DXR-induced lethal toxicity. Between these two, OLV were significantly less toxic at the two highest DXR doses tested (20 and 25 mg/kg).

(C4) Anti-tumor activity of liposome-associated and free DXR

The enhanced therapeutic effect of L-DXR in the J6456 metastatic tumor model [6] has been correlated

TABLE II

Toxicity of doxorubicin in free and liposome-associated form in BALB/c male mice

Experimental group [a]	Dose (mg/kg)	Median survival (range) [c]	60-day survival (%)	180-day survival (%)
OLV	25	>180 (56- >180)	80	60
SUV	25	2 (1- 2)	0	0
Free	25	6 (5- 8)	0	0
OLV	20	>180	100	100
SUV	20	2 (1- 12)	0	0
Free	20	5 (8- 9)	0	0
OLV	18 [b]	>60	100	–
SUV	18 [b]	51 (26- >60)	60	–
Free	18 [b]	7 (4- 11)	0	–
OLV	15	>180	100	100
SUV	15	>180	100	100
Free	15	73 (10- >180)	60	40

[a] i.v. single injection of DXR in either free, SUV or OLV form. Each group consisted of five mice.

[b] In this group, the observation period was 60 days only.

[c] Statistical significance (Wilcoxon test): $P < 0.01$ for OLV vs. SUV at 25 and 20 mg/kg; OLV vs. Free at 25, 20 and 18 mg/kg; and SUV vs. Free at 18 mg/kg. All other comparisons were not statistically significant.

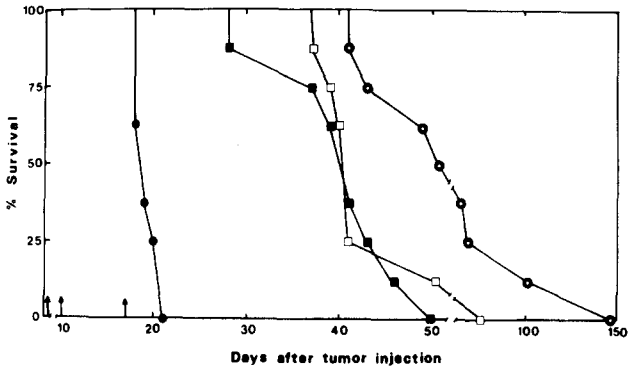

Fig. 5. A comparison of the anti-tumor activity of free DXR, DXR in SUV and DXR in OLV. BALB/c mice were inoculated i.v. with 10^6 J-6456 lymphoma cells. Arrows indicate days of treatment (3, 10 and 17 after tumor cell inoculation). Treatment was administered at the dose of 8 mg/kg for each injection (for more details see text). Free-DXR (■), OLV-DXR (○), SUV-DXR (□), untreated (●).

with an increased amount of liposome-delivered DXR to the liver [38]. Fig. 5 shows the results of treatment with F-DXR, OLV-DXR and SUV-DXR. The DXR dose (8 mg/kg, once weekly for three weeks) was the same for all three types of treatment. Treatment with OLV-DXR resulted in a significantly longer survival than with SUV-DXR or F-DXR. There was no appreciable difference in the degree of anti-tumor activity achieved with F-DXR and SUV-DXR. The increase in median life span observed with F-DXR was about 109%, compared to 138% for SUV-DXR and 270% for OLV-DXR.

Discussion

The optimization of a liposomal doxorubicin formulation for clinical use involves selection of vesicle composition, vesicle size, number of lamellae and pharmaceutically acceptable protecting agents. The combination of the above should result in a chemically and physically stable drug delivery system. The aspect of vesicle composition has been described before [6,8,9]. The effect of size and number of lamellae are the subjects of this manuscript. For this we compared two formulations which we proved are of identical composition but differing in their mean vesicle diameter and average number of lamellae. The SUV (60 nm mean diameter) are in the size range in which there are significant differences in the curvature of the two monolayers forming the bilayer [15]. This is not the case for the OLV (250 nm mean diameter) [15].

We found that OLV have a much higher loading capacity for DXR than SUV (Table I), which cannot be explained by differences in phospholipid composition, most of the drug being membrane-associated in both cases (Table I). The latter may explain why hardly any DXR was released from the vesicles by osmotic shock.

Three fluorescent techniques were used to characterize the drug in the liposomes. With all three, the SUV formulation differs from the OLV formulation, indicating that the distribution of DXR in the bilayers of the two vesicle populations is not identical.

(a) Self-quenching. DXR in the SUV show much lower self-quenching than in the OLV. This difference is related to the higher DXR mole% in the OLV bilayers (Table I). The mechanism of this self-quenching is not yet clear and can be explained by each or various combinations of the three following mechanisms: (i) Self-quenching results from self-association of DXR in the surface of the vesicle as described previously for dipalmitoyl-PC SUV [39]. It is worth noting that self-quenching in the case of dipalmitoyl-PC occurs at DXR to phospholipid mole ratio of 1 mole% [39], while no self-quenching occurs in PC/PG/Chol SUV, even at 2 mole% DXR. This may be due to the negative charge of PG which cause a more even distribution of DXR in the bilayer surface than in the neutral surface of dipalmitoyl-PC. (ii) The large content of DXR in the OLV bilayer makes it a bilayer component significant enough to change the local environment of the DXR in the lipid bilayer which is responsible for the quenching observed. Similar observation was made for dehydroergosterol in which increasing its bilayer concentration increases the dielectric constant of its local environment [40]. (iii) The third possibility is self-quenching due to energy transfer. The exact self-quenching mechanism may be resolved by measuring the concentration-dependent fluorescence emission life-time of DXR.

(b) Collisional quenching. The large difference in Stern-Volmer coefficient (K_{SV}) for quenching of DXR by the membrane impermeable quencher iodide between OLV and SUV (K_{SV} of 1.6 and 10.8 M^{-1}, respectively) suggests much higher exposure of DXR to the quencher in the SUV. Theoretical predictions based on the difference in number of lamellae per vesicle suggest that the ratio between accessible fractions of fluorophores in the two vesicle populations should be 2.0 at the most and not the observed K_{SV} SUV/K_{SV} OLV ratio of 6.75. The difference between predicted and observed ratio can be explained in two different ways: (i) It is related to curvature difference between the SUV and OLV. The small radius of curvature of the SUV causes major differences in packing of their phospholipid molecules between the outer and inner monolayers [15]. This results in asymmetric distribution of DXR, with most of the drug present in the outer monolayer. In the OLV, due to the larger radius of curvature which is similar in all lamellae, the DXR is evenly distributed between all four monolayers. Under such conditions a maximal ratio of K_{SV} SUV/K_{SV} OLV of 4.65 is expected. This value is still lower than the observed ratio of 6.75. (ii) An additional or alternative explanation is that DXR is localized deeper in the

OLV bilayer than in the SUV bilayer and is therefore less exposed to the quencher.

(c) Rotational mobility. Steady-state fluorescent anisotropy of DXR also indicates drastic differences in DXR rotational mobility between OLV and SUV. This observation may be related to concentration-dependent self-quenching, as in the case of dehydroergosterol [40], where changes in r due to self-quenching were of the same magnitude as in our system. Alternatively, changes in the local environment of DXR caused by drug/lipid phase separation or by a deeper insertion of the drug molecules into the hydrophobic part of the lipid bilayer may reduce, in the case of OLV, the strong electrostatic interaction between DXR and PG which may be part of the restriction to DXR rotation at the lipid/water interface of SUV.

Correlation between physical and pharmacological characteristics

The reduced stability of SUV-DXR association as opposed to OLV-DXR appears to be the result of two physical attributes of the vesicles: (i) Differences in number of lamellae per vesicle. (ii) Differences in curvature which affect the packing of the lipids in the bilayer and may determine DXR organization in the bilayer: SUV have a tightly packed head group region in their inner leaflet, while in the outer leaflet this packing is disordered [15]. Thus, most DXR molecules which are associated with the polar region of the bilayer [31] will distribute into the outer leaflet of the vesicle. This asymmetric head group packing may explain the enhanced penetration of serum apolipoprotein into the SUV [42,43], which could destabilize DXR–phospholipid interaction on the vesicle surface. This could lead to high plasma peaks of free drug which account for increased toxity [41]. The differences in physical characteristics result in a higher level of DXR exposure to the external environment in SUV (approx. 7 fold), which may be related to the differences in the pharmacology of the two liposome formulations. As shown here, the pattern of biodistribution of OLV and SUV were significantly different, while that of the latter was similar to that of free DXR.

Our data indicate that most of the OLV-DXR is cleared by liver and spleen, which are the main organs responsible for clearance of large liposomes [10,11]. The increased drug levels in the liver may explain superior antitumor activity of OLV-DXR when compared to SUV-DXR and free DXR in a tumor model with dominant liver involvement. Another important consequence of the difference in organ biodistribution is that for OLV-mediated delivery of DXR there is a decrease in drug concentration in toxicity-related organs such as cardiac muscle, small intestine and kidneys [7] (Fig. 4). The overall effect is a concomitant improvement in efficacy against liver tumors and reduction in toxicity, namely a gain in therapeutic index.

Our data stress the relevance of the vesicle physical properties, in the optimization of liposomal formulations, and specifically, the pharmacological implications of vesicle size and number of lamellae in the design of DXR containing liposomes for clinical use. These studies were instrumental in the selection of a formulation of liposomal DXR for use in Phase I clinical trial [44,45].

Acknowledgements

This work was supported by the Robert Szold Fund for Applied Science (Jerusalem, Israel), and by Liposome Technology, Inc. (Menlo Park, CA, U.S.A.).

References

1 Rahman, A., Kessler, A., More, N., Sikic, B., Rowden, G., Woolley, P. and Schein, P.S. (1980) Cancer Res. 40, 1532–1537.
2 Rahman, A., White, G., More, N. and Schein, P.S. (1985) Cancer Res. 45, 769–803.
3 Forssen, E.A. and Tokes, Z.A. (1981) Proc. Natl. Acad. Sci. USA 78, 1873–1877.
4 Olson, F., Mayhew, E., Maslow, D., Rustum, Y. and Szoka, F. (1982) Eur. J. Cancer Clin. Oncol. 18, 167–176.
5 Van Hoesel, Q.G., Steerenberg, P.A., Crommelin, D.J., Van Dijk, A., Van Oort, W., Klein, S., Douze, J.M., DeWildt, D.J. and Hillen, F.C. (1984) Cancer Res. 44, 3698–3705.
6 Gabizon, A., Goren, D., Fuks, Z., Meshorer, A. and Barenholz, Y. (1985) Br. J. Cancer 51, 681–689.
7 Gabizon, A., Meshorer, A. and Barenholz, Y. (1986) J. Natl. Cancer Inst. 77, 459–469.
8 Gabizon, A., Dagan, A., Goren, D., Barenholz, Y. and Fuks, Z. (1982) Cancer Res. 42, 4734–4739.
9 Gabizon, A., Goren, D., Ramu, A. and Barenholz, Y. (1986) in Targeting of Drugs with Synthetic Systems (Gregoriadis, G., Senior, J. and Poste, G., eds.), pp. 229–238, Plenum Press, New York.
10 Senior, J.H. (1987) Crit. Rev. Ther. Drug Carrier Systems 3, 123–193.
11 Hwang, K.J. (1987) in Liposomes, From Biophysics to Therapeutics (Ostro, M.J., ed.), pp. 109–156, Marcel Dekker, New York.
12 Freise, J., Muller, W.H., Brolsch, C.H. and Schmidt, F.W. (1980) Biomedicine (Paris) 32, 118–123.
13 Poste, G., Bucana, C., Raz, A., Bugelski, P., Kirsh, R. and Fidler, I.J. (1982) Cancer Res. 42, 1412–1422.
14 Papahadjopoulos, D. and Gabizon, A. (1986) Ann. N.Y. Acad. Sci. 504, 64–74.
15 Lichtenberg, D. and Barenholz, Y. (1988) in Methods in Biochemical Analysis (Glick, D., ed.), Vol. 33, pp. 337–462, Wiley, New York.
16 Storm, G., Steerenberg, P.A., Emmen, F., Van Borssum Waalkes, M. and Crommelin, D.J.A. (1988) Biochim. Biophys. Acta 965, 136–145.
17 Barenholz, Y., Gibbs, D., Litman, B.J., Goll, J., Thompson, T.E. and Callson, F.D. (1977) Biochemistry 16, 2806–2810.
18 Klein, R.A. (1970) Biochim. Biophys. Acta 210, 486–489.
19 Samuni, A., Chong, P.L.-G., Barenholz, Y. and Thompson, T.E. (1986) Cancer Res. 46, 594–599.

20 Takanashi, S. and Bachur, N.R. (1976) Drug. Metab. Dispos. 4, 79–87.
21 Druckmann, S., Gabizon, A. and Barenholz, Y. (1989) Biochim. Biophys. Acta 980, 381–384.
22 Bartlett, G.R. (1959) J. Biol. Chem. 234, 466–468.
23 Stewart, J.C. (1980) Anal. Biochem. 104, 10–14.
24 Dijkstra, J., Van Galen, W.J.M., Hulstaert, C.E., Kalicharan, D., Roerdink, F.H. and Scherphof, G.L. (1984) Exp. Cell Res. 150, 161–176.
25 Goll, J., Carlson, F.D., Barenholz, Y., Litman, B.J. and Thompson, T.E. (1982) Biophys. J. 38, 7–13.
26 Nordlund, J.R., Schmidt, C.F., Dickens, S.N. and Thompson, T.E. (1981) Biochemistry 20, 3237–3244.
27 Bligh, E.G. and Dyer, W.J. (1959) Can. J. Biochem. Physiol. 37, 911–917.
28 Menozzi, M., Valentini, L., Vannini, E. and Arcamone, F. (1984) J. Pharm. Sci. 73, 766–770.
29 Lakowciz, J.R. (1983) Principles of Fluorescence Spectroscopy. Plenum Press, New York.
30 Eftink, M.R. and Ghiron, C.A. (1981) Anal. Biochem. 114, 199–227.
31 Burke, T.G. and Tritton, T.R. (1985) Biochemistry 24, 5972–5980.
32 Shinitzky, M. and Barenholz, Y. (1978) Biochim. Biophys. Acta 515, 367–394.
33 Litman, B.J. and Barenholz, Y. (1982) Methods Enzymol. 81, 678–685.
34 Bachur, N.R., Moore, A.L., Bernstein, J.G. and Liu, A. (1970) Cancer Chemother. Rep. 54, 89–94.
35 Gabizon, A. and Trainin, N. (1980) Br. J. Cancer 42, 551–558.
36 Gabizon, A., Goren, D. and Barenholz, Y. (1986) J. Cell. Biochem. 10B, 82.
37 Ben Yashar, V. and Barenholz, Y. (1989) Biochim. Biophys. Acta 985, 271–278.
38 Gabizon, A., Goren, D., Fuks, Z., Barenholz, Y., Dagan, A. and Meshorer, A. (1983) Cancer Res. 43, 4730–4735.
39 Burke, T.G. and Tritton, T.R. (1984) Anal. Biochem. 193, 135–140.
40 Schroder, F., Barenholz, Y., Gratton, E. and Thompson, T.E. (1987) Biochemistry 26, 2441–2448.
41 Legha, S.S., Benjamin, R.S., Mackay, B., Eewer, M., Wallace, S., Valdivieso, M., Rasmussen, S.L., Blumenschein, G.R. and Freireich, E.J. (1982) Ann. Intern. Med. 96, 133–139.
42 Wetterau, J.A. and Jonas, A. (1982) J. Biol. Chem. 257, 10961–10966.
43 Bonte, F. and Juliano, R.L. (1986) Chem. Phys. Lipids 40, 359–372.
44 Amselem, S., Gabizon, A. and Barenholz, Y. (1990) J. Phar. Sci., in press.
45 Gabizon, A., Peretz, T., Sulkes, A., Amselem, S., Ben Yosef, R., Ben-Baruch, N., Catane, R., Biran, S. and Barenholz, Y. (1989) Eur. J. Cancer Clin. Oncol. 25, 1795–1803.
46 Barenholz, Y. et al. (1991) Med. Res. Rev., in press.